IDENTIFYING OCCUPANTS' APPROPRIATE SEATING POSITION AND VIEW DIRECTION IN OFFICE BUILDINGS: A STOCHASTIC SHADE CONTROL BASED MULTI-OBJECTIVE VISUAL COMFORT OPTIMIZATION

Jian Yao[1]

ABSTRACT

Manually operated solar shades have a significant impact on indoor visual comfort. This research investigates occupants' appropriate seating position and view direction in a west-facing office cell using a previously developed shade behavior model. The non-dominant sorting genetic algorithm (NSGA-II) based Multi-objective optimization was adopted to identify the optimal and near optimal solutions. Daylight and glare index were used as two visual comfort objectives for optimization and robustness of optimization results against shade behavior uncertainty that was analyzed using statistical analysis. Results show that near optimal solutions can be used instead of the optimal one since they provide more flexibility in seating positions while maintaining almost the same visual comfort performance. And thus, the appropriate seating position considering occupants' preference is 1.5m away from the external window with two view directions near parallel to the window for west-facing office rooms.

KEYWORDS

manual solar shades, occupant behavior, visual comfort, Multi-objective optimization, seating position

1. INTRODUCTION

Daylighting contributes significantly to occupant perceptions of well-being within buildings [1] as well as benefits, such as lighting energy savings [2] and a high productivity level due to increased visual comfort [3]. Thus, modern architecture favours buildings with large ratios of glazing to floor areas for admitting sufficient daylight into indoor spaces [4], which also brings negative impacts on indoor environmental quality such as glare problems and increased cooling demands [3]. To balance daylighting performance and glare protection, roller shades are widely used in glazed-office buildings in the hot summer and cold winter zone of China. The use of solar shades provides occupants with individual control over their own indoor comfort conditions and thus reduces lighting and cooling/heating energy consumption [5].

1. Department of Architecture, Ningbo University, Ningbo, China, yaojian@nbu.edu.cn

Daylight performance has been widely investigated by researchers. For example, Esquivias et al. [6] performed a daylight simulation of shading devices in an office building and different types of fixed shading were considered including overhangs, side fins, horizontal and vertical louvres. They concluded that that these fixed shading devices are not efficient in controlling dynamic daylight illuminance due to the excessive reduction in the daylight illuminance range of 500 and 2000 lux. Similar studies have been reported in the literature [7, 8]. Although automated solar shading systems have been used to improve the daylighting performance in many studies [3, 9, 10], Meerbeek et al. [11] reported there is a tendency that in the control mode with manual override capability occupants are more satisfied with the visual conditions than in the automated control mode.

Daylight glare protection is another important index for improving indoor visual comfort. Visual discomfort and glare rating assessment of integrated daylighting and electric lighting systems were investigated by Apiparn et al. [12]. An anidolic daylighting system combined with several electric lighting fixtures was measured and different glare rating indexes including daylight glare index (DGI), daylighting glare probability (DGP) and unified glare rating (UGR) were calculated by using high dynamic range (HDR) imaging techniques. Similar studies based on HDR measurement were conducted to evaluate indoor visual conditions and identify the source of discomfort glare [13–15].

Daylighting performance and/or glare protection have also been investigated along with indoor thermal and energy performance. For example, Lartigue et al. [16] conducted Multi-objective optimization of the building envelope considering both energy consumption and daylighting performance. Different window to wall area ratios and window types were considered and the optimal non-dominated solutions were calculated using the Pareto method. Yao [17, 18] measured and simulated the daylighting/glare and thermal performance before and after using roller solar shades in residential and office buildings. His research indicated that movable solar shades play a significant role in improving indoor thermal and visual conditions in the hot summer and cold winter zone of China.

Due to the dynamic nature of sky conditions, occupants' shade control are complex and stochastic [5, 19, 20], and thus the indoor visual condition at different seating positions with different view directions varies with time during the year [21]. Therefore, the selection of appropriate seating positions and view directions for office buildings with manual shades will be a challenging task. To achieve a high indoor visual performance at a seating position during the whole year, there are generally three possible ways: (1) changing the way occupants behave (solar shade control behavior) to respond to external sky conditions efficiently since previous research studies show occupant behavior with solar shades is not efficient (e.g. forget to reopen solar shades for increasing indoor daylight levels when glare sources disappear) [22]; (2) use of automated shading systems for highly efficient control of solar shades to overcome the drawbacks of occupants' behavior as described above; (3) selecting appropriate seating positions and view directions based on occupants' shade control behavior. Previous research has indicated that changing occupants' behavior using strict control may decrease their tolerance for greater variation in indoor environmental conditions [23] and may negatively affect productivity. While for automated systems, Reinhart and Voss [24] found that in 88% of the cases when the blinds were lowered automatically, occupants manually raised them within 15 min, indicating automated systems do not satisfy users (partly due to the lack of understanding of occupants' preference for daylight levels). Therefore, the last possible way (selecting appropriate seating positions and view directions based on occupants' shade control behavior), which is less sensitive to occupant

behavior and does not require additional mechanical systems, will be a low cost and robust design strategy for achieving a high indoor visual condition. However, identifying appropriate seating positions and view directions is a complex and challenging task that involves balancing illuminance and glare since such factors are dynamic and depend on sun position, sky conditions and occupants' uncertainty over shade control, which means the identified solution should be robust to occupant behavior. Here robust means that there should be a converged solution (the optimal or near optimal solutions) for repeated shade behavior simulations whatever shade behavior changes given the same behavior model.

Although daylighting performance and glare risks of roller shades have been investigated in several research studies [15, 17, 25–27], most of them are based on automated or ideal control modes and neither of them are based on realistic occupant behavior with shades and over an annual simulation performance. For example, Kong et al. [28] measured and simulated the impact of interior design (seat position and view direction etc.) on visual discomfort reduction. They found that seating orientations towards windows and adjacent to windows lead to a higher rate of glare risks. However, the research was based on automated shading systems controlled by solar radiometers and photometric sensors and thus the conclusion may not be applicable to manually controlled shades. Recently, Bian et al. [29] proposed a discomfort glare evaluation method based on the concept of 'adaptive zone' through rotating view direction and shifting seating position. A simulation was conducted for bare windows and fixed shading devices (overhang shading and light shelf shading). They found that the introduction of the concept of 'adaptive zone' in visual comfort predictions significantly reduces both the degree and the occurring time of discomfort glare.

Most office buildings located in the hot summer and cold winter zone of China use manual roller shades due to its much lower cost compared to automated ones and thus there is a need to investigate the appropriate seating position and view direction based on occupants' stochastic control of roller shades, rather than ideal control modes as described above. The current work is an extension of previous studies which focus on the evaluation of daylighting performance and glare risks at a fixed seating position [21, 30] and the focus is to identify the optimal and near optimal solutions for indoor seating position and view direction of west-facing office rooms in the hot summer and cold winter zone of China based on stochastic control of manual shades using Multi-objective optimization.

2. METHODOLOGY

2.1 Shade Behavior Model

To investigate the impact of manual solar shades on indoor visual comfort, the stochastic model of manual solar shades developed in a previous study by the author [5] was used in this research. The model was constructed based on field measurements on an office building in the hot summer and cold winter zone of China. In this model, occupants' shade control was divided into 5 solar shading states (shade window area of 0%, 25%, 50%, 75% and 100%, respectively, which means the occupant can adjust solar shades to any of these 5 positions randomly. Then, a first order and time-constant Markov chain method was used to develop the stochastic model of solar shade control, and the Markov chain transition matrix (the probability of solar shade changes from the current state to the next position) for different sky conditions were calculated and classified according to the determined driving factor (solar radiation). More detailed information of this stochastic model can be found in paper [5]. This behavior model was created in

FIGURE 1. A graphic illustration of the co-simulation framework for the stochastic shade behavior model.

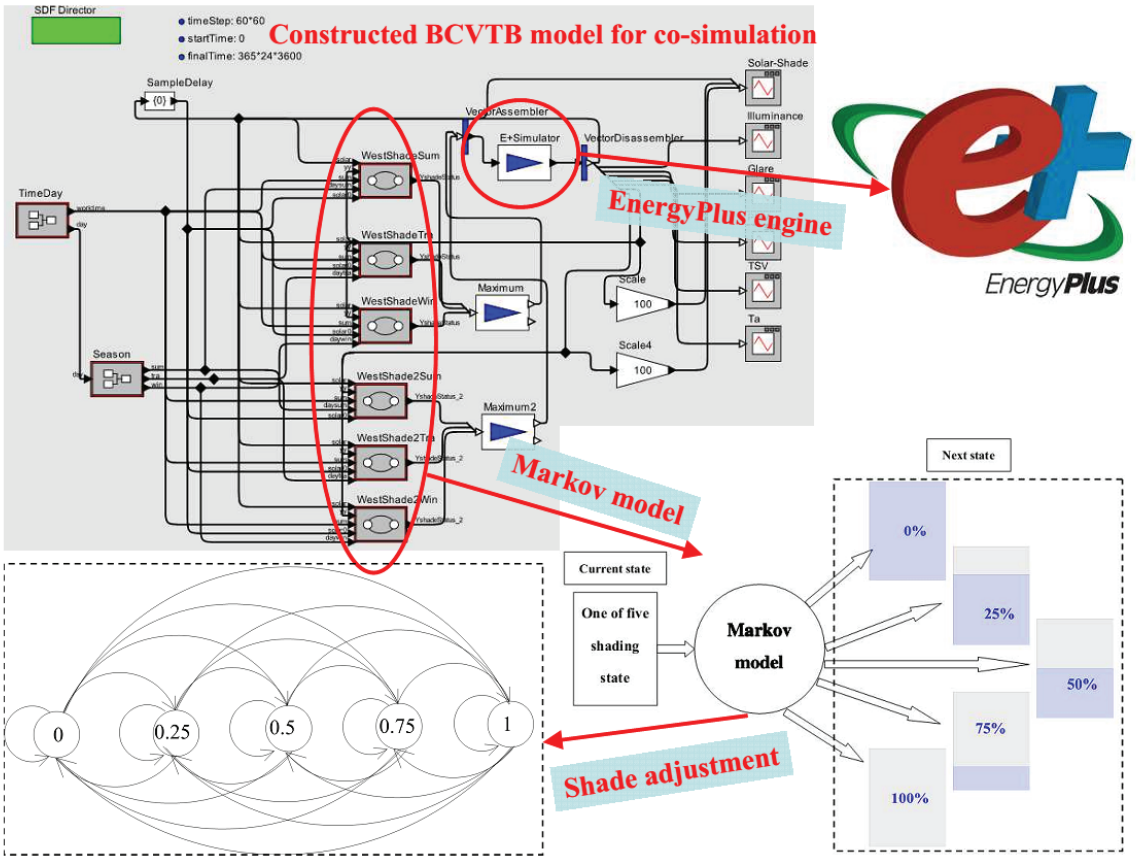

a building controls virtual test bed (BCVTB), a software environment developed by Lawrence Berkeley National Laboratory and allows expert users to couple different simulation programs [31], for co-simulation with EnergyPlus and a graphic illustration of this co-simulation framework is shown in Figure 1. The co-simulation results (shade control action (SC values described in section 2.4.1) at each time step (each hour during the year)) were generated and used for simulation-based optimization.

2.2 Typical Office Cell

The research was conducted for a typical office cell (see Figure 2a) in Ningbo (a typical city in the hot summer and cold winter zone of China). Its dimension is 4 × 4 × 3m with a 3.8 × 2.8m window on the west facade. The characteristics of the office cell are shown in Table 1. The material property of roller solar shades was collected from a local manufacturer.

2.3 Optimization Method

2.3.1 Optimization setting

To compare the indoor visual performance of manual solar shades at different seating positions and view directions, the combination of three design variables was considered. Table 2 shows

TABLE 1. Characteristics of the office cell.

Parameter	Value
Location	Ningbo city, latitude: 30°,longitude: 120°
Room orientation	West
Dimension	Room: 4 × 4 × 3m, Window: 3.8 × 2.8m
Window and shading device	Clear double-pane window +manually controlled roller shades with visual transmittance: 0.2 (beam: 0.04, diffuse: 0.16), reflectance: 0.7(Specular: 0; diffuse: 0.7); roughness:0.01; Five shade positions: Percentage of shaded window area of 0%, 25%, 50%, 75% and 100%
Surface reflectance	Wall: 0.75, ceiling: 0.75, floor: 0.25

the considered three design variables for optimization. The first variable is view direction at seating position, which mainly influences daylight glare protection. As can be seen in Figure 2b, there are a total of 24 directions considered with an interval of 15 degrees. Each direction corresponds to the middle of a roughly 60 degree view cone. The other two parameters are related to the location of the seating position (x and y values as can be seen in Table 2), and thus a two dimensional grid at workplane height was considered with a grid space of 0.5m (that meets the requirement of the Illuminating Engineering Society of North America (IESNA) 2012 [32]), leading to a total of 49 (7 × 7) possible seating positions inside the office cell. Therefore, there were 1176 (49 × 24) possible design solutions to explore considering the combination of these three design variables. For comparison, a smaller grid of 0.1m spacing was simulated to validate the accuracy of the above grid size in identifying the optimal and near optimal solutions. Although some of potential solutions might be pre-filtered for the studied office cell (e.g. a seating position of 0.5m from interior walls though staring at the wall is not desirable), this optimization technique is a general method for such kind of analysis and has its advantages for larger offices with more complex room geometry and facade design while a simple pre-filter technique cannot easily be applied to such cases.

In the current study, two objectives were set to identify the appropriate solutions. The first objective is related to daylighting performance and thus the useful daylight illuminance (UDI) index was used, which determines when illuminance levels are beneficial for the occupant, that

TABLE 2. Design variables for optimization.

Parameter	Values	Number of options
Orientation (North Axis, degree)	0, 15, 30, 45, . . ., 345	24
X location (room depth, m)	0.5, 1, 1.5, 2, . . ., 3.5	7
Y location (room width, m)	0.5, 1, 1.5, 2, . . ., 3.5	7
Total options		1176

FIGURE 2. Possible seating positions and view directions.

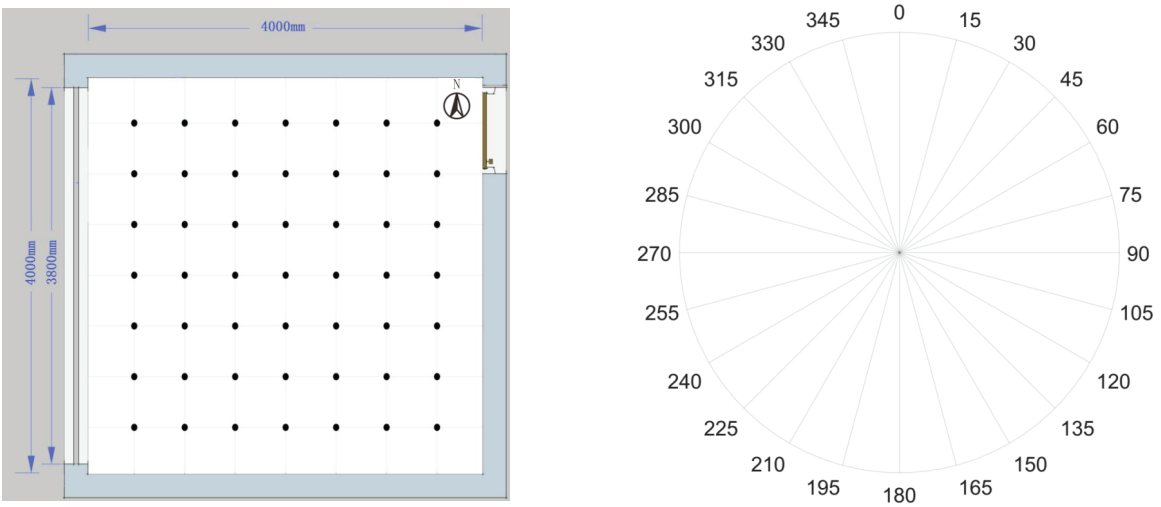

(a) 49 possible seating positions inside the office

(b) 24 possible view directions

is, more than 300 lx [33] (not too dark) and less than 2000 lx (not too bright) [34]. Too much daylight in the view field leads to glare risks. The other objective is related to glare protection and daylight glare index (DGI) [35] which was considered rather than daylight glare probability (DGP) since DGP cannot be predicted with the simulation engine described below. Optimization objectives are to minimize the time of DGI over 22 (22 is the maximum allowable DGI value for visual comfort [12]) and the time of UDI outside the range of 300–2000lux. The minimization of these two objectives leads to an optimal indoor visual comfort performance—a maximum daylighting performance and a minimum glare risk. These two objective functions denoted as "UDI_unmet_time," which corresponds to a maximum daylighting performance, and "DGI_unmet_time," which corresponds to a minimum glare risk, can be expressed as follows:

min (UDI_unmet_time) and min (DGI_unmet_time)

where

$$\mathrm{UDI\_unmet\_time}\left(\mathrm{Pt}_i\right) = \sum_{j=1}^{8760} \mathrm{H}\left(\mathrm{L}\left(\mathrm{Pt}_{i,j}\right)\right) \tag{1}$$

$$\mathrm{DGI\_unmet\_time}\left(\mathrm{Pt}_i\right) = \sum_{j=1}^{8760} \mathrm{K}\left(\mathrm{L}\left(\mathrm{Pt}_{i,j}\right)\right) \tag{2}$$

Where L(·) represents the simulation result, which is the output of the simulation for sampling point i (one of the 1176 possible options described in Table 2) and time j (within a year from 1

to 8760). H(·) and K(·) are two functions that are calculated based on the daylight illuminance value and DGI value and can be expressed as follows:

$$H(x) = \left\{ \begin{array}{c} 0, \text{ if } 300 \le x \le 2000 \\ 1, \text{ otherwise} \end{array} \right\} \tag{3}$$

$$K(x) = \left\{ \begin{array}{c} 0, \text{ if } x \le 22 \\ 1, \text{ otherwise} \end{array} \right\} \tag{4}$$

When simulating UDI, a workplane height of 0.8m was considered, while for DGI a height of 1.2m (at seated occupants' eye height level) was set in the simulation. In general, heating or cooling related thermal performance is not influenced by seating position and view direction. Thus, thermal related objectives are not considered. The optimal seating position and view direction depend on the dynamic usage of roller shades during the whole year, rather than just a time point or a short period of time. Consequently, the optimal solution will be identified based on the annual simulation results. In addition, near optimal solutions (solutions with the simulated two objective indexes being slightly higher than the optimal solution) will also be analyzed for providing occupants with both similar indoor visual performance to the optimal one and a flexibility of seating position and view direction. It should be noted that the influences of screen glare, view to outdoor and occupants' shadow onto their own work are not considered since they cannot be simulated by EnergyPlus.

2.3.2 Optimization algorithm

Since occupant behavior with solar shades is stochastic, repeated simulations are required to capture performance uncertainty due to behavior uncertainty. The following analysis (see section 3.1) has shown that 25 repeated simulations achieve a convergence of simulation results; therefore, a total of 1176 × 25 = 29400 simulations are required to identify the optimal and near optimal solutions. To reduce the simulation time, optimization analysis instead of a full parametric simulation was considered and the non-dominant sorting genetic algorithm (NSGA-II) [36] was used for Multi-objective optimization since it is a robust and versatile optimization algorithm [37]. The setting of this algorithm is that the max generation (the number of iterations of the optimization) is 200; the population size (the number of solutions to be evaluated in each iteration) is 10; the crossover rate (how often the new solutions are created by merging features of existing solutions) is 1; the mutation rate (how often random changes happen to the new solutions) is 0.2; and the tournament selection size (new solutions in Evolutionary Algorithms are created from selected existing solutions) is 2. These settings are in line with the calibration of this tool with a full parametric study [38].

The optimization tool (jEPlus+EA), which uses the simulation engine EnergyPlus developed by the U.S. Department of Energy (DOE) [39] for building performance simulation, was adopted to conduct the above optimization analysis. jEPlus+EA is an open source tool originally developed for managing complex parametric simulations, which is coupled with optimization algorithms such as Evolutionary Algorithms (EA) [40]. It has been widely used for building performance optimization and calibration [38, 41, 42]. Since the optimization was based on annual indoor visual performance, typical weather year data for Ningbo city was used for hourly simulation.

2.4 Robustness of Optimization Solutions

2.4.1 Uncertainty of occupant behavior

Due to the stochastic characteristics of occupant behavior, shade control varies between occupants, and even the same occupant at the same environmental condition he/she may have different control actions at different times of year. Consequently, the shade behavior model as described in section 2.1 produces different shade control actions between repeated whole year simulations. Accounting for uncertainty of occupant behavior requires a certain number of repeated simulations to be conducted and compared for the relationship between each two replications. To assesses how well the relationship between two replications (here hourly shading coefficient (SC) values between different simulations were considered since SC directly related to the covering percentage of the window, e.g. a SC of 0.25 represents 75% of window area was covered by shades), the index correlation coefficient was considered, which varies between +1 and –1. A value of +1 indicates a perfect positive correlation between the two variables, –1 represents a totally negative correlation and 0 corresponds to an absence of linear correlation. In general, a weak correlation of hourly SC values between repeated simulations indicates a relatively high uncertainty of occupant behavior. Since SC values are discrete and ordinal (SC values: 0, 0.25, 0.5, 0.75 and 1), Spearman rank correlation [43], a non-parametric test, was used for statistical calculation. The Spearman rank correlation test does not carry any assumptions about the distribution of the data and thus is appropriate for correlation analysis for SC values. It can be expressed as follows:

$$r = \frac{\mathrm{cov}\left(rg_{sci}, rg_{scj}\right)}{\sigma_{rg_{sci}} \sigma_{rg_{scj}}} \tag{5}$$

where cov(·) is the covariance of the rank variables (SC values: 0, 0.25, 0.5, 0.75 and 1) and $\sigma_{rg_{sci}}$, $\sigma_{rg_{scj}}$ are the standard deviations of the rank variables, and i, j are the number of repeated simulation described below.

2.4.2 Number of repeated simulations

Due to the uncertainty of shade behavior, different shade control actions based on the same shade behavior model (as described in section 2.1) should be considered to check the robustness of the optimization results. Different shade control actions can be generated by repeated co-simulation of the stochastic behavior model described in Figure 1. To determine the minimal number of repeated simulation, the graphical method, a simple graphical approach that plots the cumulative mean of the simulation output data, suggested by [44] was used. After sufficient replications, the graph will become a flat line with no upward or downward trend. The number of replications required is defined by the point at which the line becomes flat.

2.5 Comparison with Simplified Shade Control Modes

Due to complexity of modeling shade control behavior in annual building performance simulation, manual solar shades are mainly treated as automated systems or simplified control modes in building performance simulation without considering the stochastic characteristics of occupant behavior. For example, in research by Tzempelikos et al. [45], solar shades were automatically closed if external solar radiation exceeds 120 W/m^2. While Reinhart [46] assumed that

solar blinds were closed if solar radiation on the façade exceeds 50 W/m^2. Sometimes, manual shades are even treated as fully open or fully closed in performance simulations neglecting their dynamic nature in controlling solar radiation. These rigid and fixed thresholds cannot reflect the stochastic nature of occupant behavior and may lead to a biased evaluation of indoor visual performance, seating positions and view directions. Therefore, the appropriate seating positions and view directions identified based on a shade behavior model were compared with two typical automated shade controls (the two fixed solar radiation thresholds described above: 50 W/m^2 and 120 W/m^2) and with two simple control modes (fully open and fully closed for the whole year respectively) in order to determine their capabilities of identifying the optimal and near optimal solutions as the behavior model. Although a limited number of studies reported shade behavior models [47, 48], these models cannot be applied directly to a hot summer and cold winter zone of China due to the difference in climate characteristics, shade control modes and shading materials etc. Thus, these manual control models are not compared in this research.

3. RESULTS AND DISCUSSION

3.1 Behavior Uncertainty

Figure 3 presents Spearman correlation coefficient of annual hourly SC values between the 25 replications. The areas of circles shown in this figure represent the absolute values of corresponding correlation coefficients. The larger the areas of circles are, the stronger the correlation between replications. It can be seen that on the principal diagonal the areas of circles are the

FIGURE 3. Spearman correlation coefficient of annual hourly SC values between the 25 replications (N1 . . . N25 represent replication1 . . . replication25).

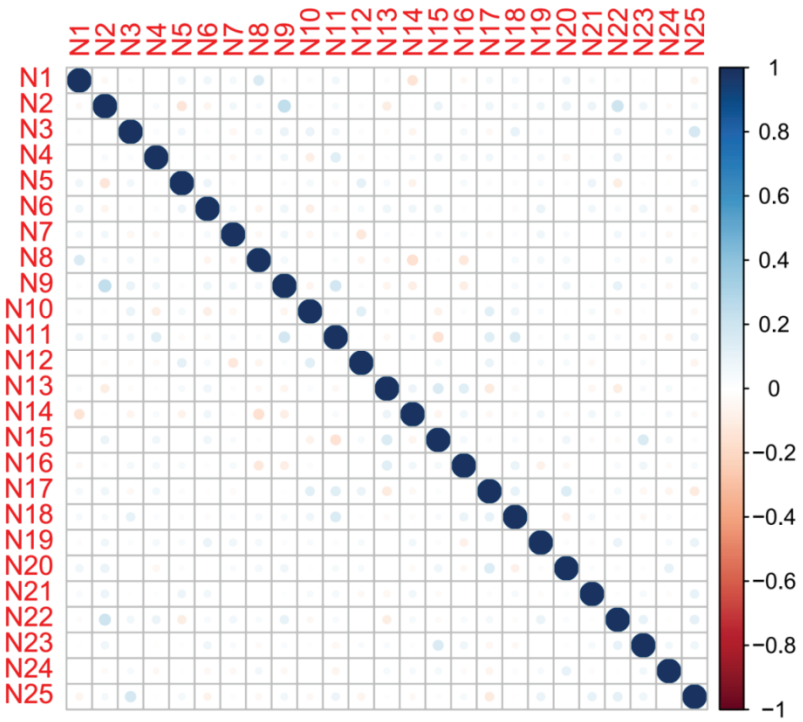

FIGURE 4. Annual average SC values between the 25 replications.

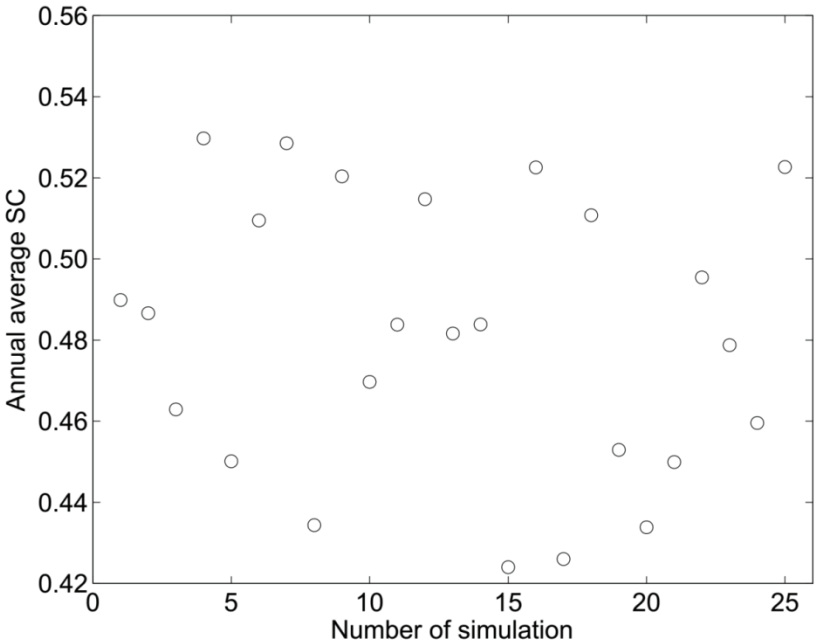

largest with a Spearman correlation coefficient of 1, which is due to the fact that the calculation is based on the same SC value sequence (such as N1 vs. N1). However, the correlation coefficients for other situations (off diagonal elements) are close to 0 with only a few values reaching about 0.1/–0.1. In statistics, a correlation coefficient in the range of [–0.19, 0.19] indicates no or a very weak relationship [49]. Therefore, Figure 3 shows that there is no or a very poor relationship between 25 replications of occupant behavior in terms of hourly SC value sequence, indicating occupant uncertainty was not suppressed by the behavior model. Figure 4 further gives annual average SC values between the 25 replications, which range from about 0.43 to 0.53, indicating behavior uncertainty can be produced on an annual basis by the shade behavior model and thus indoor visual performance uncertainty should be considered in the following analysis.

To determine how many simulation replications are needed to reduce performance uncertainty due to behavior uncertainty, the graphical method described in section 2.4.2 was used to check the convergence of UDI unmet time (the optimal solutions for different replications all have the same DGI unmet time of 0 as shown in the following analysis and thus there is no need to do a convergence check for this index) and the result is shown in Figure 5. It can be seen from the figure that the results converge at about 20 replications with a 95% confidence interval. Performing more replications beyond this point will only give a marginal improvement in the estimation of the mean value. Meanwhile, the maximum difference of the confidence interval is only 0.67% after 25 replications, a very small value (means a high accuracy) for daylighting prediction and thus 25 replications were selected for the following uncertainty analysis.

3.2 Optimization Result

Figure 6 presents Multi-objective optimization results for the shade behavior model for one of the 25 replications with red points indicating the optimal solutions, which have both the

FIGURE 5. Convergence of UDI unmet time prediction. The solid line indicates the mean value while the dashed lines indicate the 95% confidence interval.

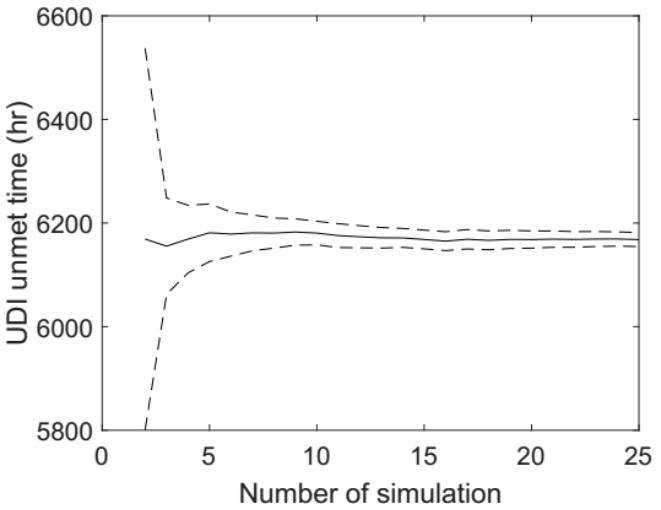

minimal DGI unmet time and minimal UDI unmet time. It can be seen that for different combinations of the three design variables both DGI unmet time and UDI unmet time vary significantly, indicating a large performance deviation between different solutions. For example, the DGI unmet time ranges from 0 to about 3500 hr while the UDI unmet time ranges from about 6100 to about 7300 hr. Through optimization, the optimal solutions have been identified

FIGURE 6. Multi-objective optimization results for the shade behavior model. (The scatter plot shows all of the explored solutions for one of the 25 replications, with those in the current population (blue) and the current optimal solutions (red) marked.).

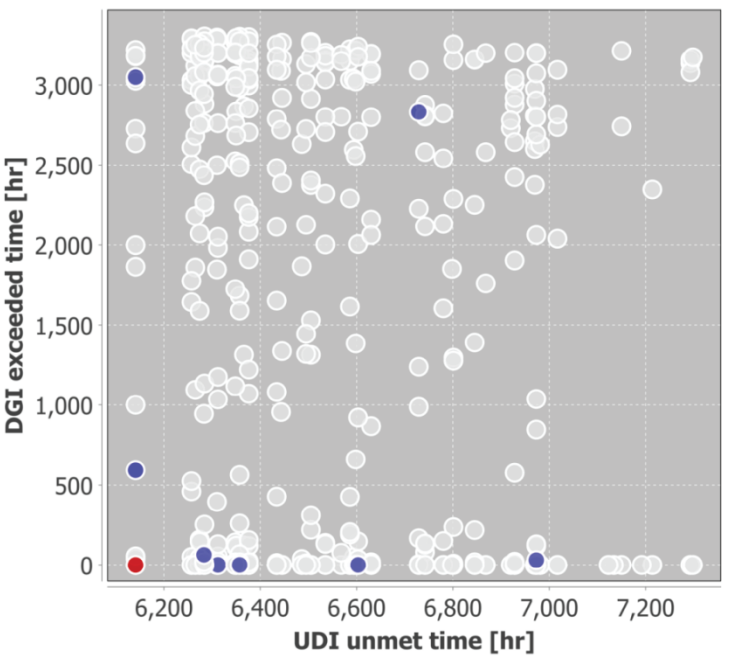

with the minimal DGI unmet time being 0 hr and the minimal UDI unmet time being 6141 hr, corresponding to 2169 working hours (8760h in a year and thus 8760 – 6141 = 2619) meeting UDI criterion (2619/3650 = 71.7% of working time which assumes 10 hr per day (365day × 10h = 3650)).

Figure 7 shows the convergence line for the above optimization problem, and it can be seen that after 40 generations (less than the setting: 200 generations) the best solutions have been identified. To further validate the reliability of optimization results, a parametric analysis of the simulation replication was conducted and all possible combinations (the whole searching space, 1176 simulations are described in Table 2) were simulated and the same optimal solutions were identified as the optimization method. Therefore, the optimization algorithm is capable of identifying the true optimal solutions.

In addition, the influence of the size of grid spacing on the optimal solution was analyzed using a new optimization with a smaller grid space of 0.1m, leading to a total of 1444 (38 × 38) possible seating positions. The results show that the difference of optimal seating position is only 0.2m, indicating an acceptable level of accuracy of the above analysis (the grid size of 0.5m).

3.3 Robustness of the Best Solutions

The best solutions for the 25 simulation replications according to Multi-objective optimization are illustrated in Figure 8. It can be seen that there are only two best seating points for the 25

FIGURE 7. Convergence line for the optimization problem for the replication illustrated in Figure 6.

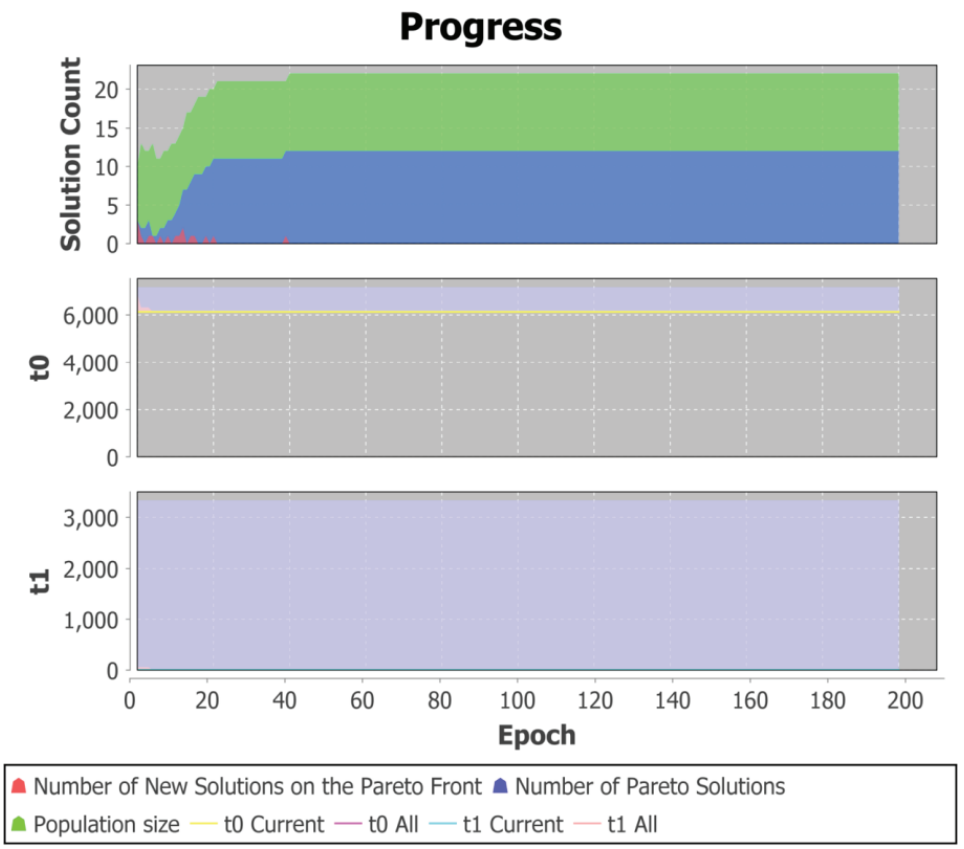

replications with the x,y locations of (1.5m, 0.5m) or (2.0m, 0.5m). For the best view direction shown in Figure 8(b), all 25 replications have the same optimization result of 11 view directions ranging from 30 to 180 degrees. Other points or view directions all lead to a poorer performance in terms of daylighting and glare protection. Since these 11 best solutions have continuous viewing angles, the best view direction can be considered any angle in the range of 30 to 180 degrees. Although there are two best seating positions rather than one, most solutions (20/25 × 100% = 80%) suggest the location of (1.5m, 0.5m) with the same view directions and the difference between the two points is small. Therefore, this position (1.5m, 0.5m) with a view direction of ranging from 30 to 180 degrees (from the direction of northeast to south) can be considered the best solution in terms of daylighting and glare protection with high robustness against occupant behavior uncertainty.

In addition to the optimal seating location and view direction, the uncertainty of UDI unmet time and DGI unmet time was also analyzed to determine how robust these optimal solutions are. Figure 9 illustrates a normal probability plot of UDI unmet time for the 25 simulation replications. It can be seen that the data points are near the red straight line (a theoretical normal distribution), indicating the normality of the data which was further validated by using a rigorous statistical test (Kolmogorov-Smirnov test). Therefore, the two parameters (the mean value = 6168 hr and standard deviation = 32 hr) were obtained through fitting normal distribution to the data points. For uncertainty analysis, the 95% confidence interval was used and the corresponding uncertainty range is [6104, 6232] hr, which is a very narrow range and thus the UDI performance is robust. While for DGI unmet time, these 25 optimization results

FIGURE 8. The optimal solutions with seating position and view directions for the 25 replications.

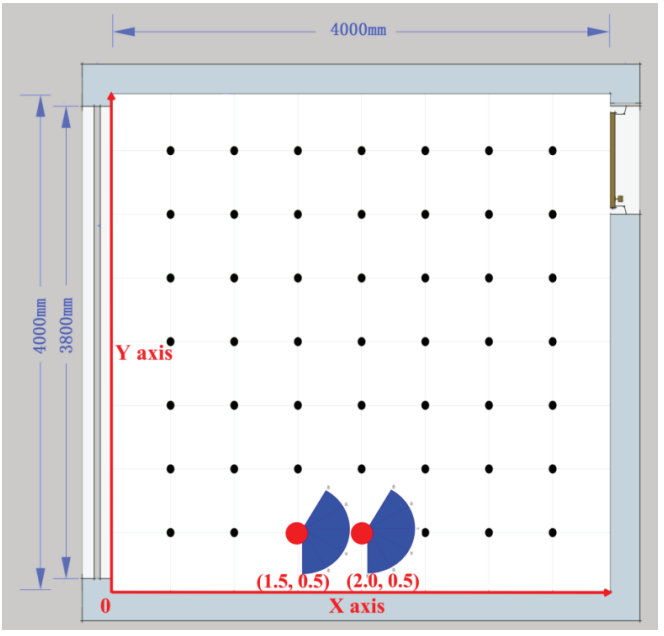

(a) Optimal seating positions (the red points show the locations of the seating position) and view directions (blue region which is enlarged and presented below)

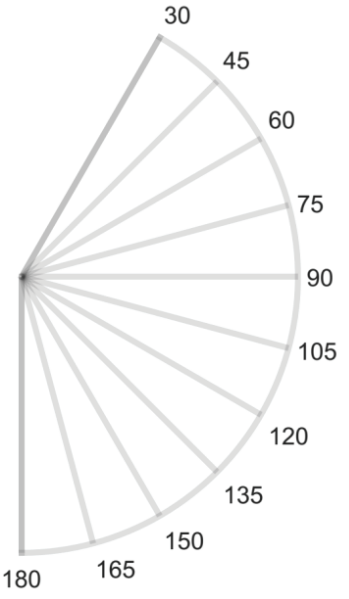

(b) 11 optimal view directions

FIGURE 9. Normal probability plot of UDI unmet time for the 25 simulation replications.

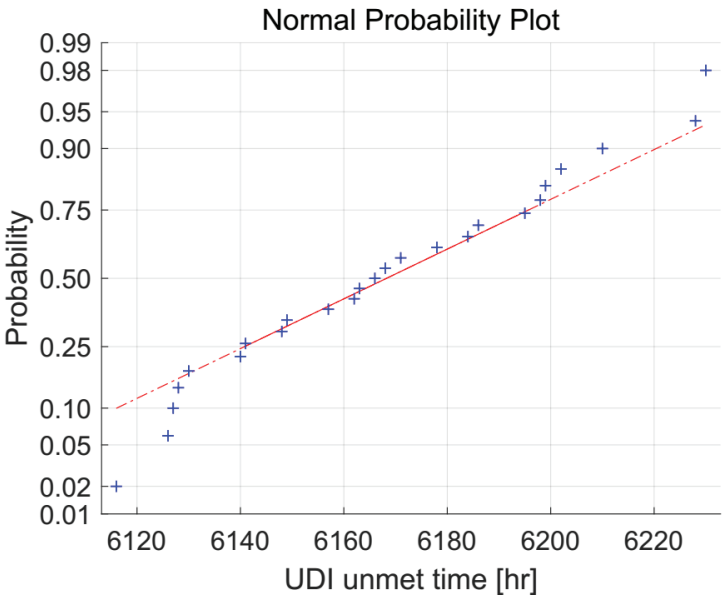

are all 0, indicating a more robust performance than UDI. Therefore, the visual performance of the optimal solutions is robust and not sensitive to occupant uncertainty of shade control.

3.4 Comparison

3.4.1 The optimal solution

The four simplified shade controls were simulated and optimization results as well as a comparison with the behavior model are listed in Table 3 and Figure 10. It can be seen that for the optimal solution and the fully open mode the optimal position is close to the behavior model with a difference of 0.5–1.0m on the x axis and the best view directions are the same as the behavior model. The solar threshold 50W/m^2 is also close to the behavior model but with the best seating position closer to the window due to the use of solar shades when solar intensity exceeds 50W/m^2.

On the other hand, for the fully closed mode, the best seating position (near the middle of the room) is far (about 2m away) from the behavior model and a small deviation (15 degrees) of the range of optimal view directions. For the control mode of solar threshold 120W/m^2, the optimal solution is in the middle of the office cell plane, which is far (about 1.4m away) from the low solar intensity mode (50W/m^2) and (about 1.6m away) from the behavior model. Meanwhile, there is a very small difference (about 15 degrees) for the optimal view direction compared to the behavior model.

Beside the optimal solution, UDI unmet time of the behavior model is much higher than the other shade control modes with a deviation of 2.7–17.2%. That means currently used shade control modes in building performance simulation may overestimate the UDI performance if UDI was simulated at the optimal seating position. While for DGI unmet time, these four control modes have the same optimization result (0 hr) as the behavior model. This is because the view directions are mainly away from the external window for all of these shade control modes.

Therefore, selecting the optimal seating position and view direction for manual controlled solar shades based on the modes of fully closed and solar threshold 120W/m^2 leads to a discrepancy while the choices based on fully open and solar threshold 50W/m^2 seems to be acceptable although a little difference may exist (UDI performance may be overestimated by 6.6% or 13.9% depending on the choice of selected shade control mode).

A clear conclusion that can be drawn from the optimization is that the optimal view direction is away from the window. It also can be seen that all of these optimal solutions are at the middle region of the office cell and near the south façade. That means a relatively small seating region inside a typical office cell, where optimal visual comfort is achieved, can be recommended for typical solar shade control systems. However, the above analysis also indicates that different control modes of solar shades lead to different optimal seating positions and view directions, which means there is a need to carefully select seating positions if a highest visual comfort condition is required.

3.4.2 Near optimal solutions

The above analysis of the optimal solution focused on the best single point. However, it seems that there are still a few points near the optimal solution as can be seen in Figure 6 (a few grey points near the red point which are near optimal solutions), indicating a similar or a little poorer performance which may also be acceptable. Therefore, further investigation of the map of UDI unmet time distribution for different control modes was conducted and the results are shown in Figure 11 (sub-figures do not have values at one or two points (Figure 11(a) and (e)) is due to the sampling technique used by the NSGA-II optimization algorithm and this does not influence the searching of optimal and near optimal solutions by the algorithm). It can be seen that for the behavior model there are a few near optimal solutions at the location

TABLE 3. Comparison of different shade control modes with the behavior model in terms of optimal solutions as well as the minimal values of corresponding objectives.

	Shade control mode				
	Behavior model	**Fully open**	**Fully closed**	**Solar threshold: 50W/m^2**	**Solar threshold: 120W/m^2**
Optimal seating position [m]	80% probability: (1.5, 0.5) 20% probability: (2.0, 0.5)	(2.5, 0.5)	(1.0, 2.0)	(1.0, 1.0)	(2.0, 2.0)
Optimal view direction [degree]	30–180	30–180	15–165	30–180	15–150
UDI unmet time [hr]	95% CI: [6104, 6232]	5759	6000	5309	5108
DGI unmet time [hr]	0	0	0	0	0
Deviation of UDI unmet time from behavior model	0	6.6%	2.7%	13.9%	17.2%

Note: the optimal seating position is expressed in terms of x, y location

FIGURE10. Comparison of different shade control modes with the behavior model in terms of optimal solutions (the red point shows the location of the seating position and blue regions represent view directions).

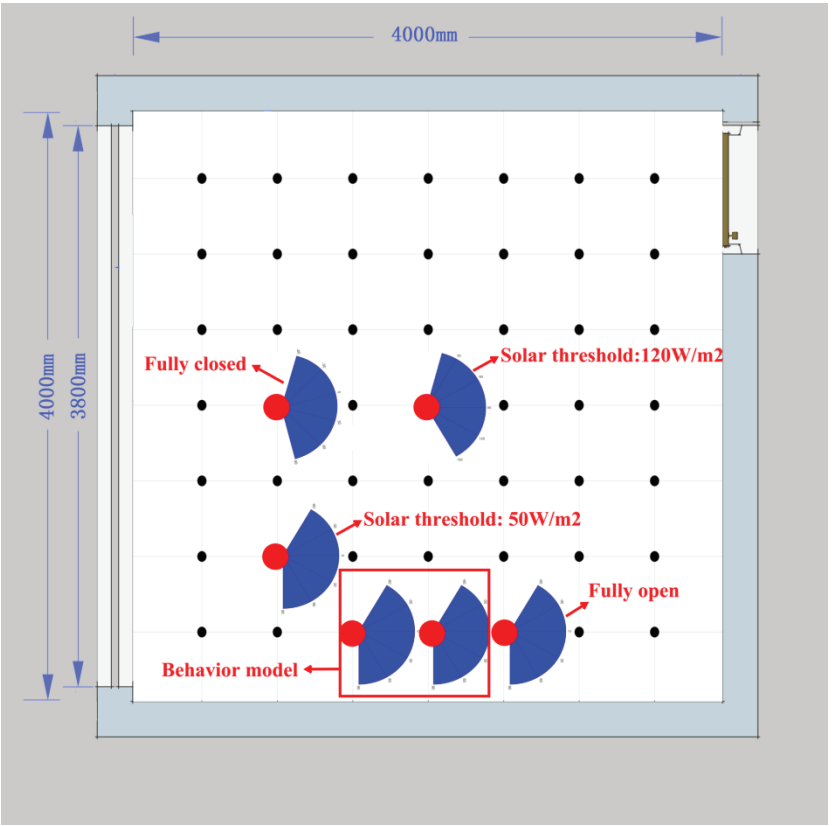

of about x = 1.5–2m and y from 0.5 to 3.5m (here x and y are the axes illustrated in Figure 8 which represent the room depth and room width respectively) with a maximum difference of UDI unmet time of 3.9%.

While for the view direction, a range of about 15 to 165 degrees (a deviation of about 15 degrees compared to the optimal solution) lead to a DGI unmet time of 0. Therefore, near optimal solutions have a relatively small performance difference compared with the single optimal solution, indicating that these near optimal solutions can be adopted in order to provide occupants with a flexibility of seating position (more seating positions compared to the optimal one) while maintaining approximately the same level of indoor visual performance. In addition, near optimal solutions for the 25 replications almost have the same seating region and view directions (see Figure 12), indicating a robust performance of these solutions against behavior uncertainty. Therefore, the appropriate seating positions (1.5–2m away from the window) and view directions (15 to 165 degrees, from the direction of northeast to southeast) for the west facade based on the above analysis can be determined according to near optimal solutions which are given in Figure 12. In reality, most occupants prefer to sit near windows with an outside view in the view field and thus a reasonable and practical solution according to Figure 12 would be seating positions in the blue rectangle with two view directions marked with red arrows (15 and 165 degrees in Figure 12). These two view directions are suggested since they are nearly

FIGURE 11. Map of UDI unmet time distribution for different control modes.

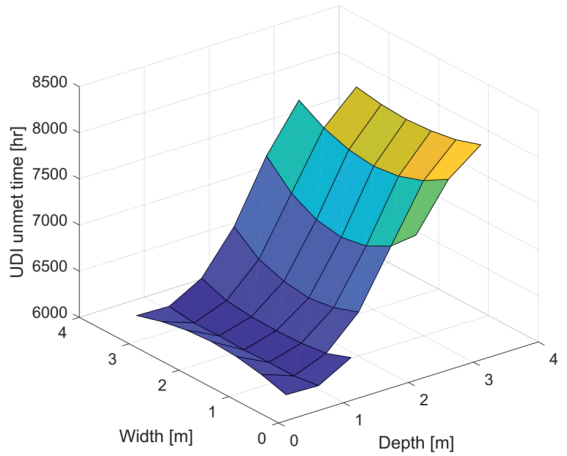

(a) fully closed mode

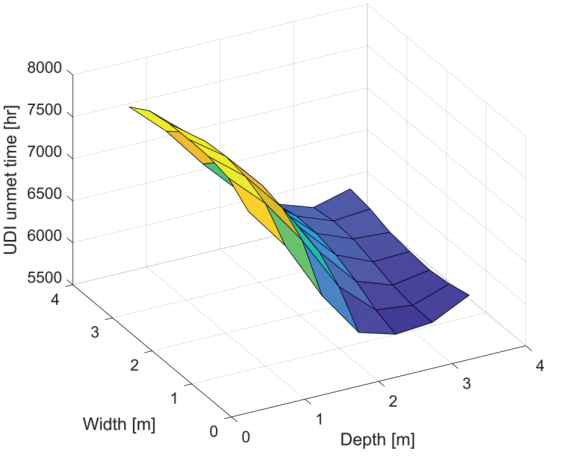

(b) fully open mode

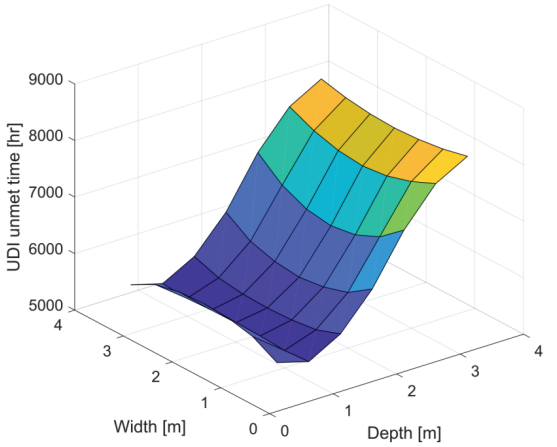

(c) solar threshold 50 W/m^2

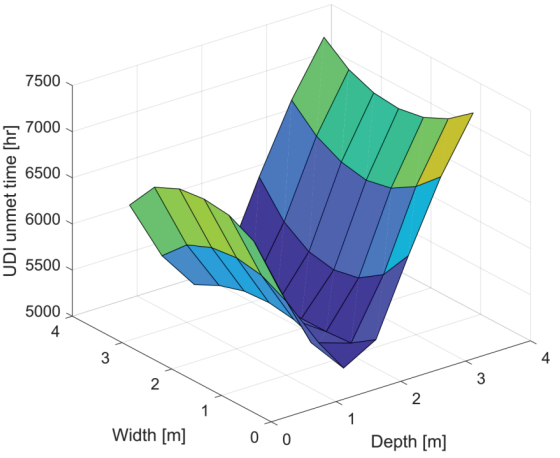

(d) solar threshold 120 W/m^2

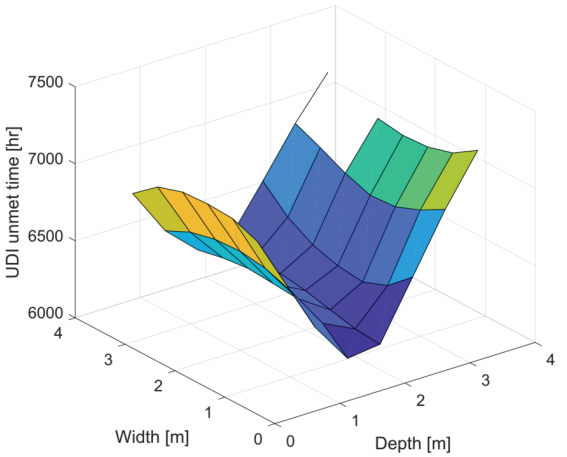

(e) one of the simulation replication of the behavior model

parallel to the window (occupants do not face the back wall) and thus occupants can easily have a view to the outdoors by adjusting a small amount of view direction. In addition, these two view directions help reduce the likelihood of veiling glare on a computer monitor which does not face the window. Therefore, the seating positions about 1.5m away from windows with two view directions near parallel to the window are practically optimal for most occupants.

Interestingly, it is found in Figure 12 that the near optimal solutions are symmetric. This is mainly due to the fact that the two shades were adjusted according to the same stochastic model and the annual trend of adjustment of these two shades is similar although large differences exist at hourly scales. Therefore, the annual daylighting and glare performance at these points are similar and consequently, symmetrically near optimal solutions are identified.

Although the deviation (see section 3.4.1) of UDI unmet time from the behavior model for solar threshold 120W/m^2 is higher than the other modes in terms of the single optimal solution, this difference does not necessarily indicate that the identified near optimal solutions are also farther from the behavior model than the other three simplified modes. Instead, it can be seen that for these simplified shade control modes only solar threshold 120W/m^2 has a similar curved surface of the UDI unmet time distribution, indicating that they have similar are near optimal solutions (seating positions). In addition, the aim of the above comparison is to check the effectiveness of these simplified shade control modes in identifying appropriate seating positions and view directions as the shade behavior model rather than finding a simplified mode that has a minimal UDI unmet time difference compared to the shade behavior model. Therefore, the solar threshold 120W/m^2 mode can be considered to represent the shade behavior model

FIGURE 12. Appropriate seating positions and view directions (points inside the red rectangle indicate near optimal seating positions with each point having the same view direction ranging from 15 to 165 degrees).

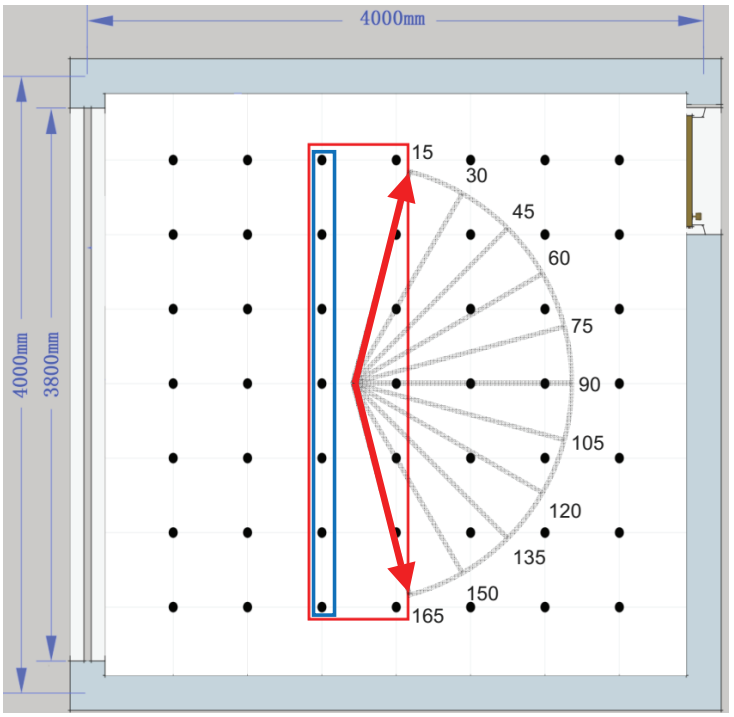

for selecting appropriate seating positions and view directions. This means that using simplified shade control modes for identifying suitable seating positions and view directions is not an easy task and requires a careful selection of appropriate simplified control modes.

As can be seen from Figure 12, near optimal solutions provide more choices of seating positions compared to the single optimal solution and thus are more likely to be accepted by occupants with different preferences for seating positions. Meanwhile, the visual performance of near optimal solutions is almost as high as the optimal one and thus in some cases they can be considered as the best solutions since occupants' adaptation to visual conditions can extend the limit of comfort range of UDI and glare indexes. This research is useful for interior design (such as the layout of office tables) of glazing office buildings in China and its findings can help designers avoid inappropriate seating positions. In addition, the proposed methodology is general and can be used in other cases with any window size at any location and orientation.

4. CONCLUSIONS

Manual solar shades are widely used in office buildings in China due to their lower costs compared to automated ones. The performance of such kind of shades highly depends on occupant behavior, which is complex and stochastic. Thus, performance prediction based on simulation using simple assumptions may deviate from actual performance and lead to a wrong decision in selecting appropriate furniture layout. This research investigates occupants' optimal and near optimal seating position and view direction in a west-facing office cell based on the behavior model on solar shades developed by the author and NSGA-II algorithm based Multi-objective optimization was used to identify the optimal solution. Four simplified solar shade control modes (two based on solar threshold and the other two are fully open and fully closed respectively) were compared to determine their effectiveness of identifying optimal and near optimal solutions in representing the behavior model.

Results show that the appropriate seating position can be determined using near optimal solutions and its location is 1.5m away from the external window with two view directions near parallel to the window (occupants do not face the back wall) and thus is capable of having a view outside. Although the solar threshold 120W/m^2 mode is a little poorer than other control modes with regard to the single optimal solution, near optimal solutions of this mode are closer to the behavior model compared to other modes and thus this mode is more likely to be accepted by occupants since near optimal solutions provide more flexibility in seating positions without a significant reduction of indoor visual comfort. Therefore, a solar threshold of 120W/m^2 can be considered to represent the behavior model for selecting appropriate seating position and view direction. Since the current research only considered four simplified shade control modes, other control modes may have a better performance than the solar threshold 120W/m^2 for representing shade control behavior and this needs to be further investigated.

The findings of this research are based on the shade behavior model developed in the hot summer and cold winter zone of China and thus its applicability to other climate regions or different window sizes/orientations may be limited. Meanwhile, it should be noted that the appropriate seating positions and view directions suggested for the west facade are based on the two (UDI and DGI) selected visual related indexes and may be building specific (such as ratios of glazing to wall areas and physical properties of solar shades). However, the methodology used in this research is general and can be applied to other similar studies with any window size at any location and orientation.

This research is based on optimization of objective visual comfort indexes, occupants' subjective perception of indoor visual comfort and other psychological and physiological factors are not considered such as view (which is a very important factor in selecting seating position and view direction), user preferences (e.g. solutions for different users—one who likes more view and will tolerate more glare; one for a user that wants even lighting and is mainly working on paper etc.) and multiple occupants in open-plan offices with different preferences. Therefore, further research is required to conduct more detailed investigation by including not only objective and quantitative indexes but also occupants' subjective and qualitative factors. Meanwhile, future simulation studies and field measurements are required to further compare the effectiveness of controlling daylight levels and glare protection of manual shades with other passive and active solutions in order to provide improvement suggestions on manual shade control as well as design strategies for shading devices.

Acknowledgement

This work was supported by the National Natural Science Foundation of China under Grant No. 51878358, Natural Science Foundation of Zhejiang Province under Grant No. LY18E080012, and National Key Technology R&D Program of the Ministry of Science and Technology under Grant 2013BAJ10B06. The author also would like to thank the K.C.Wong Magna Fund at Ningbo University.

REFERENCES

[1]. Clevenger, C.M. and Z. Rogers, Managing Daylight in Airports. Journal of Architectural Engineering, 2017. 23(3): article number 04017006.

[2]. Lynes, J.A. and P.J. Littlefair, Lighting energy savings from daylight: estimation at the sketch design stage. Lighting Research and Technology, 1990. 22(3): p. 129–137.

[3]. Koo, S.Y., M.S. Yeo and K.W. Kim, Automated blind control to maximize the benefits of daylight in buildings. Building and Environment, 2010. 45(6): p. 1508–1520.

[4]. Feuermann, D. and A. Novoplansky, Reversible low solar heat gain windows for energy savings. Solar Energy, 1998. 62(3): p. 169–175.

[5]. Yao, J., Determining the energy performance of manually controlled solar shades: A stochastic model based co-simulation analysis. Applied Energy, 2014. 127(8): p. 64–80.

[6]. Esquivias, P., et al., Climate-based daylight analysis of fixed shading devices in an open-plan office. Lighting Research and Technology, 2016. 48(2): p. 205–220.

[7]. Stazi, F., et al., Comparison on solar shadings: Monitoring of the thermo-physical behaviour, assessment of the energy saving, thermal comfort, natural lighting and environmental impact. Solar Energy, 2014. 105: p. 512–528.

[8]. Freewan, A.A.Y., Impact of external shading devices on thermal and daylighting performance of offices in hot climate regions. Solar Energy, 2014. 102: p. 14–30.

[9]. Nielsen, M.V., S. Svendsen and L.B. Jensen, Quantifying the potential of automated dynamic solar shading in office buildings through integrated simulations of energy and daylight. Solar Energy, 2011. 85(5): p. 757–768.

[10]. Kim, J., et al., An experimental study on the environmental performance of the automated blind in summer. Building and Environment, 2009. 44(7): p. 1517–1527.

[11]. Meerbeek, B., et al., Building automation and perceived control: A field study on motorized exterior blinds in Dutch offices. Building and Environment, 2014. 79(8): p. 66–77.

[12]. Borisuit, A., J.L. Scartezzini and A. Thanachareonkit, Visual discomfort and glare rating assessment of integrated daylighting and electric lighting systems using HDR imaging techniques. Architectural Science Review, 2010. 53(4): p. 359–373.

[13]. Konis, K., Predicting visual comfort in side-lit open-plan core zones: Results of a field study pairing high dynamic range images with subjective responses. Energy and Buildings, 2014. 77: p. 67–79.
[14]. Yun, G., K.C. Yoon and K.S. Kim, The influence of shading control strategies on the visual comfort and energy demand of office buildings. Energy and Buildings, 2014. 84: p. 70–85.
[15]. Konstantzos, I., A. Tzempelikos and Y. Chan, Experimental and simulation analysis of daylight glare probability in offices with dynamic window shades. Building and Environment, 2015. 87: p. 244–254.
[16]. Lartigue, B., B. Lasternas and V. Loftness, Multi-objective optimization of building envelope for energy consumption and daylight. Indoor and Built Environment, 2014. 23(1): p. 70–80.
[17]. Yao, J., An investigation into the impact of movable solar shades on energy, indoor thermal and visual comfort improvements. Building and Environment, 2014. 71(1): p. 24–32.
[18]. Yao, J., Effect of a novel internal roller shading system on energy performance. Journal of Green Building. 9(4): p. 125–145.
[19]. Van Den Wymelenberg, K., Patterns of occupant interaction with window blinds: A literature review. Energy and Buildings, 2012. 51: p. 165–176.
[20]. Yao, J., Stochastic Characteristics of Manual Solar Shades and their Influence on Building Energy Performance. Sustainability, 2017. 9(12): article number 1070.
[21]. Yao, J., D. Chow and Y. Chi, Impact of Manually Controlled Solar Shades on Indoor Visual Comfort. Sustainability, 2016. 8(8): article number 727.
[22]. O'Brien, W., K. Kapsis and A.K. Athienitis, Manually-operated window shade patterns in office buildings: A critical review. Building and Environment, 2013. 60: p. 319–338.
[23]. Paciuk, M., The role of personal control of the environment in thermal comfort and satisfaction at the workplace. 1989, University of Wisconsin-Milwaukee.
[24]. Reinhart, C.F., K. Voss and Others, Monitoring manual control of electric lighting and blinds. Lighting Research and Technology, 2003. 35(3): p. 243–260.
[25]. Konstantzos, I. and A. Tzempelikos, Daylight glare evaluation with the sun in the field of view through window shades. Building and Environment, 2017. 113: p. 65–77.
[26]. Shen, H. and A. Tzempelikos, Daylighting and energy analysis of private offices with automated interior roller shades. Solar Energy, 2012. 86(2): p. 681–704.
[27]. Xiong, J. and A. Tzempelikos, Model-based shading and lighting controls considering visual comfort and energy use. Solar Energy, 2016. 134: p. 416–428.
[28]. Kong, Z., et al., The impact of interior design on visual discomfort reduction: A field study integrating lighting environments with POE survey. Building and Environment, 2018. 138: p. 135–148.
[29]. Bian, Y., T. Leng and Y. Ma, A proposed discomfort glare evaluation method based on the concept of 'adaptive zone'. Building and Environment, 2018. 143: p. 306–317.
[30]. Jian, Y., Daylighting performance of manual solar shades. Light & Engineering, 2018. 26(1): p. 99–104.
[31]. BCVTB, http://simulationresearch.lbl.gov/bcvtb.
[32]. Illuminating Engineering Society, Approved method: IES spatial daylight autonomy (sDA) and annual sunlight exposure (ASE), in IESLM-83-12, Illuminating Engineering Society of North America IESNA, Illuminating Engineering Society Of North America IESNA Editors. 2012: New York.
[33]. China Academy Of Building Research, Standard for lighting design of buildings, in GB50034, China Academy Of Building Research, China Academy Of Building Research^Editors. 2013, China Architecture and Building Press: Beijing.
[34]. Nabil, A. and J. Mardaljevic, Useful daylight illuminances: A replacement for daylight factors. Energy and Buildings, 2006. 38(7): p. 905–913.
[35]. Fisekis, K., et al., Prediction of discomfort glare from windows. Lighting Research and Technology, 2003. 35(4): p. 360–369.
[36]. Deb, K., et al., A fast and elitist multiobjective genetic algorithm: NSGA-II. IEEE Transactions on Evolutionary Computation, 2002. 6(2): p. 182–197.
[37]. Shi, X., et al., A review on building energy efficient design optimization rom the perspective of architects. Renewable and Sustainable Energy Reviews, 2016. 65: p. 872–884.
[38]. Lara, R.A., et al., Optimization Tools for Building Energy Model Calibration. Energy Procedia, 2017. 111: p. 1060–1069.

[39]. Crawley, D.B., et al., EnergyPlus: creating a new-generation building energy simulation program. Energy and Buildings, 2001. 33(4): p. 319–331.
[40]. Zhang, Y., Use jEPlus as an efficient building design optimisation tool, in CIBSE ASHRAE Technical Symposium. 18: Imperial College, London UK.
[41]. Chen, X., H. Yang and K. Sun, A holistic passive design approach to optimize indoor environmental quality of a typical residential building in Hong Kong. Energy, 2016. 113: p. 267–281.
[42]. Carreras, J., et al., Multi-objective optimization of thermal modelled cubicles considering the total cost and life cycle environmental impact. Energy and Buildings, 2015. 88: p. 335–346.
[43]. Spearman, C., The proof and measurement of association between two things. Am J Psychol, 1987. 100(3–4): p. 441–471.
[44]. Robinson, S., Simulation: The Practice of Model Development and Use. 2014, UK: Palgrave Macmillan UK.
[45]. Tzempelikos, A. and A.K. Athienitis, The impact of shading design and control on building cooling and lighting demand. Solar Energy, 2007. 81(3): p. 369–382.
[46]. Reinhart, C.F., Lightswitch-2002: a model for manual and automated control of electric lighting and blinds. Solar Energy, 2004. 77(1): p. 15–28.
[47]. Haldi, F. and D. Robinson, Adaptive actions on shading devices in response to local visual stimuli. Journal of Building Performance Simulation, 2010. 3(2): p. 135–153.
[48]. Sadeghi, S.A., et al., Occupant interactions with shading and lighting systems using different control interfaces: A pilot field study. Building and Environment, 2016. 97: p. 177–195.
[49]. Prada, A., et al., Uncertainty propagation of material properties in energy simulation of existing residential buildings: The role of buildings features. Building Simulation, 2018. 11(3): p. 1–16.